Conceptual Design of Orbital Spacecraft Drone for Orbital Debris Collection for the ISS

A project presented to
The Faculty of the Department of Aerospace Engineering
San José State University

in partial fulfillment of the requirements for the degree
Master of Science in Aerospace Engineering

by

Koby F. Sin

December 2023

approved by

Dr. Periklis Papadopoulos
Faculty Advisor

ABSTRACT

Design of Orbital Spacecraft Drone for Orbital Debris Collection for the ISS

Koby F. Sin

This report entails the system level design of a conceptual spacecraft drone for orbital debris collection for the ISS. The objective of this project is to analyze the systems and subsystem level designs needed for the efficient implementation of such a spacecraft drone. This drone will operate in and out of the ISS while also being equipped with a deployable net as well as a large cargo bay and fuselage for debris collection. Object detection will be done through Earth based radar systems in order to improve ease and efficiency of the design.

Acknowledgements

I would like to thank my project advisor, Dr. Papadopoulos for his help and allowing me this opportunity to complete this project. Without him I would not have been able to have completed this project. I would also like to thank my friends and family for their continuous support throughout this process as I would not have been able to complete this without them.

Table of Contents

List of figures

List of tables

1 Introduction

1.1 Motivation

With space exploration technology continuously improving, one factor about space exploration that is a growing issue is space debris. No matter the quality of spacecraft that we launch into space, space debris can quickly derail any mission and cause critical damage to expensive components [1]. As the number of space missions continues to increase, more debris will be floating around in space, making space exploration more dangerous as time passes [1]. Space sustainability is ultimately the main goal of this project as there needs to be ways to mitigate or limit the negative effects of growing space debris. In terms of the project scope, the orbital path of the ISS is often littered with space debris that gets in the way. Oftentimes the debris can cause significant damage to any critical components in the ISS. While the ISS is a large space station that houses much complex equipment for space experimentation and exploration, proper protection of the ISS is necessary to avoid damage to expensive components on board. A spacecraft capable of docking in and out of the ISS able to collect space debris can be a beneficial solution for the protection of the ISS from space debris. Such a spacecraft will be armed with the ability to collect debris for interference avoidance as well as experimentation as well. Laser sensors installed within the spacecraft can also detect debris that can be potential dangers to collision on the ISS. Space experimentation can also be aided as well through the collection and testing of space debris, providing valuable information about the surrounding environment around the ISS.

1.2 Literature Review

1.2.1 Current Mitigations of Space Debris

Because the issue of space debris has been growing along with the increasing number of space missions, there have been many things done to limit the amount of debris being thrown into space. The US government has drafted a *National Orbital Debris Implementation Plan* which entails many different suggested ways for companies to limit their orbital debris footprint [2]. Many space agencies are also now working alongside the *Orbital Debris Interagency Working Group* to create a more sustainable future of space exploration through addressing the issue of orbital debris. Some methods include the suggestion of better designed payload separation methods that can limit debris, as well as reinforced spacecraft designs that release less debris when met with strong forces and collisions [2]. Spacecraft staging design has also been discussed in that the upper stages of a spacecraft should be designed to minimize debris by limiting accidental explosions during mission operation [3].

The European Space Agency also has the *Space Debris Mitigation Policy* which was released in 2008 detailing ways of limiting the amount of space debris entering space through improving aspects of spacecraft reentry [4]. The hope is that by 2030, there will be spacecrafts that are able to clean debris from orbit as well as have automated systems that are able to monitor space traffic to avoid future collisions that can potentially cause more debris to be created.

Ultimately, the fight against the building amounts of space debris is also a fight against the rapidly improving space technologies and the desire for exploration. There are many barriers when it comes to mitigating space debris as it is not commonly recognized worldwide as an issue [5]. On an international scale, there is no recognition of the definition of space debris and there is no true legal enforcement of any space debris laws by the Outer Space Treaty [5]. From the perspective of private companies, developments of projects regarding the removal of space debris do not inherently benefit these companies as a project regarding space debris mitigation does not grant them any resources of interest [5].

Studying the current Mitigations of space debris reveals a lot on how this issue should be tackled. The issue of space debris encompasses the broader goal of the growing problem of space debris. An understanding of how to garner interest for companies to want to tackle these is necessary for further improvement and developments on techniques to tackle this problem.

1.2.2 Previous Designs of Low Earth Orbit Spacecrafts

The goal of this project is to study the system design of our ISS spacecraft as well as take into consideration the features of past spacecraft designs. One such spacecraft design of interest is the Russian TKS spacecraft. The TKS spacecraft was a modular spacecraft which involved both the main VA spacecraft and the Functional Cargo Block (FGB) [6]. The tunneled portion near the middle right of the spacecraft connects the spacecraft and the FGB. Even though the FGB was originally used to resupply the proposed Russian Almas Space Station, the design element of the FGB can be noted for its ability to house the critical propulsion system elements of the spacecraft as well as a pressurized cargo hold. The FGB is also designed to be able to dock in and out of the VA spacecraft module and be functional on its own [6]. In relation to this project, the VA spacecraft flaunts multiple desired design elements of the proposed spacecraft in the form of its modularity and capable use of a separable and usable cargo space.

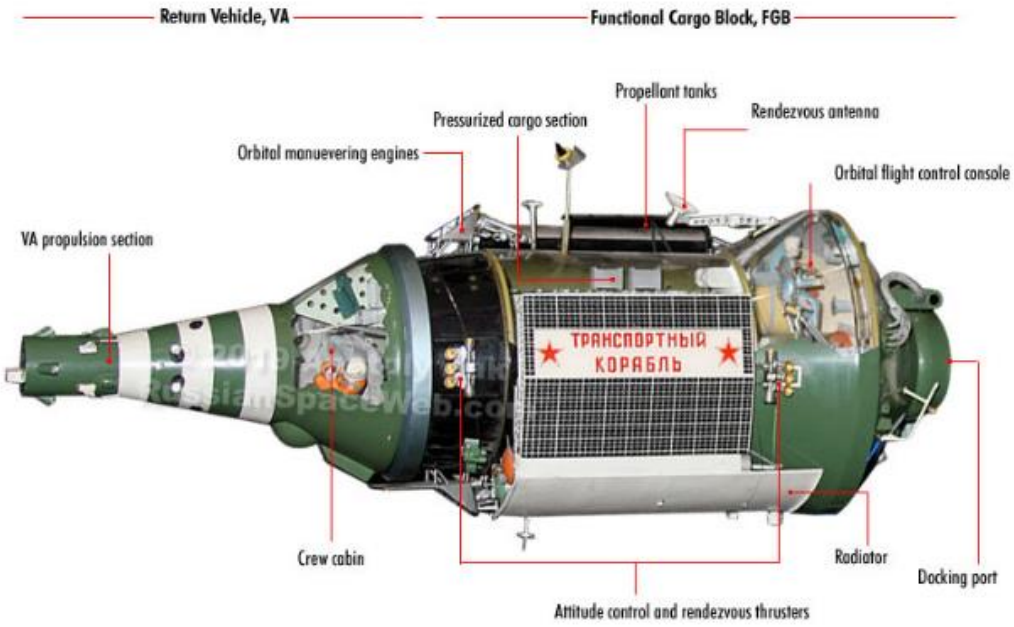

Figure 1-1 - Russian VA spacecraft with FGB module [6]

SpaceX's Dragon cargo capsule is also capable of performing missions near the ISS while being able to carry cargo along with crew members for a manned mission. With a trunk extension capable of reaching 34 m^3, this capsule can house many systems critical components as well as storage for captured debris [7]. Like the Russian TKS spacecrafts, the Dragon cargo holds are also pressurized and habitable. Its ability to integrate with the ISS through the Canada Arm as well makes it convenient for docking into the ISS, deeming it capable of resupplying a space station [15]. This would save on costs that would be needed to research and develop a separate docking station on the ISS.

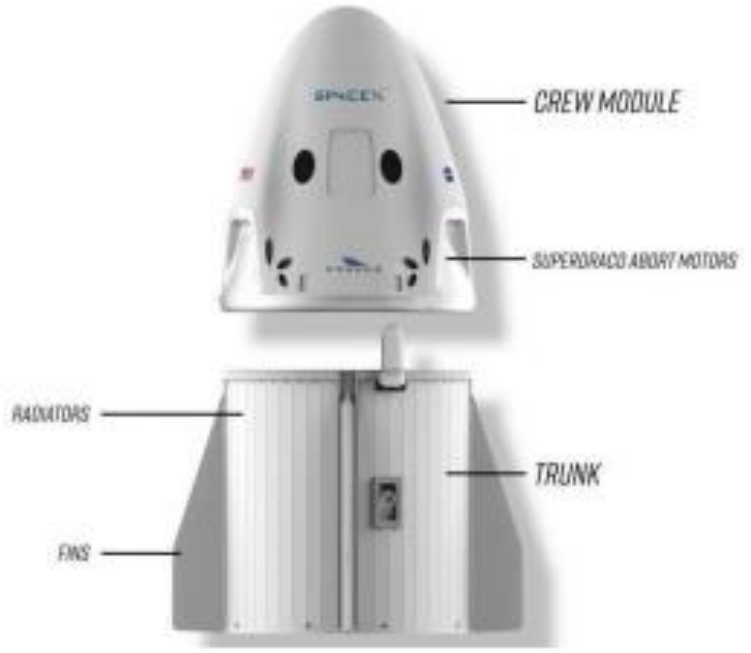

Figure 1-2 - SpaceX Dragon trunk and crew module [7]

Another worthy discussion element of the SpaceX Dragon capsule is its solar array power system. One side of the trunk capsule is lined with solar panels that provide the unit with power as well as another lithium battery pack that can power the system during times with a relative lack of sunlight [7]. The ability to house a power resource without taking additional space in the cargo hold is a design element that can benefit the proposed ISS spacecraft. Looking over the designs of the SpaceX Dragon capsule can reveal many important aspects of designing a spacecraft cargo hold and integrating it along with different modules of the spacecraft.

1.2.3 Docking Systems for Spacecrafts

Integration of the spacecraft with the ISS will be critical to the usability of the entire system. The ability of the spacecraft to dock into the ISS is critical for the convenience of the spacecraft. NASA has developed a version of the International Docking System Standard (IDSS) called the NDS that allows for docking and berthing of a spacecraft [11]. This means that any spacecraft using the IDSS can freely dock a spacecraft to the station or use a robotic arm for docking as well.

The NDS features a low approach and closed loop mating system that can also be configured for pressurized crew transfer [11]. This design is loosely based off the Russian Androgynous Peripheral Attach System (APAS) where both sides of the module can dock onto another [11]. What is important to note here is that the NDS supports power and data transfer onto the spacecraft along with docking and undocking capabilities [10]. For the scope of the project, a simple docking and undocking mechanism will be beneficial for an easy connection into the ISS. One variable to consider is that due to the extremely mechanized functionality of

such a docking system, this design requires the use of a docking adapter and will need additional power and the use of space onboard the spacecraft for this to work.

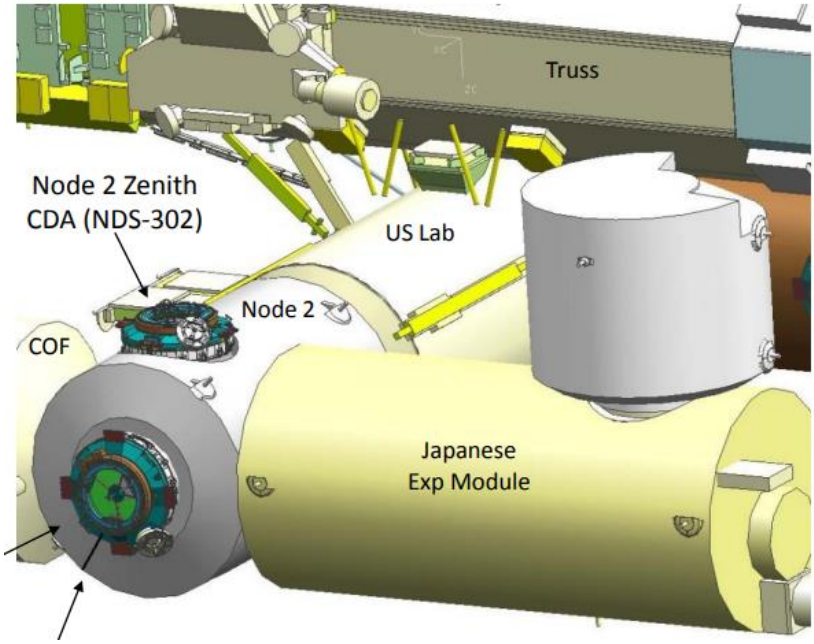

Figure 1-3 - NDS docking system with docking adapter (bottom left) [11]

Ideally, a well-designed docking system will encompass multiple feature points. NASA describes an efficient docking system as a system able to be installed within the spacecraft without taking up significant space as well as being able to withstand structural fatigue [11]. For the scope of this project, the docking system will be important to this spacecraft design as it will need to be able to integrate the cargo bay into the ISS. The docking system will also need to be designed in a manner that will not affect the overall design of the spacecraft as well. Examining different designs of docking systems will benefit the overarching goal of the project as it will give a better understanding of what different docking systems entail.

Next, we can study the design of Skylab and more importantly its design integration with the Apollo CSM module which is integrated for crew transfer from and to Skylab [8]. The Skylab included a Multiple Docking Adapter which was a hub for access into other parts of the Skylab and the Apollo spacecraft itself [8].

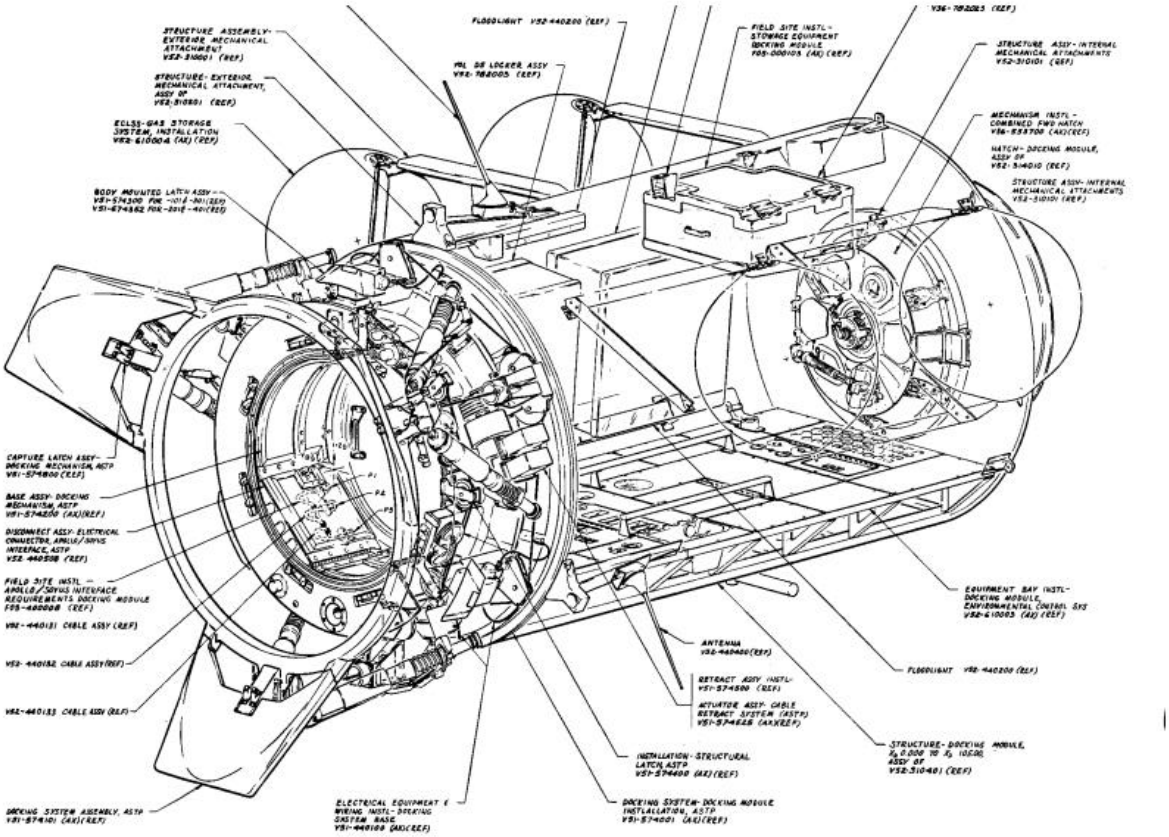

Figure 1-4 - Apollo Soyuz docking module [8]

Another version of a similar docking system for the Skylab is also the Apollo Soyuz Test Project involving the Russian Soyuz as well. Here, the docking module was designed for pressurized crew transfer in case of an emergency [8]. This allowed for easy access between different modules and could be beneficial for the project scope. The added flexibility of being able to dock across different spacecraft could prove beneficial for the usability of the project. It could ultimately be a symbol and invitation for international cooperation for the project.

Figure 1-5 - Multiple docking adapter connection into Apollo spacecraft module [8]

1.2.4 Propulsion Methods

A choice of propulsion will be necessary for this spacecraft to perform its maneuvers. Most notably there are many routes and choices of propulsion methods, and each method will have its benefits and drawbacks. The correct design and choice of propulsion methods can greatly affect the system, allowing for the spacecraft to stay functional for longer. Electronic Propulsion measures can offer engines of higher ISP and efficiency but do not offer as much thrust as chemical propulsion measures do [12]. However, this does mean that electric propulsion methods inherently offer longer burn times.

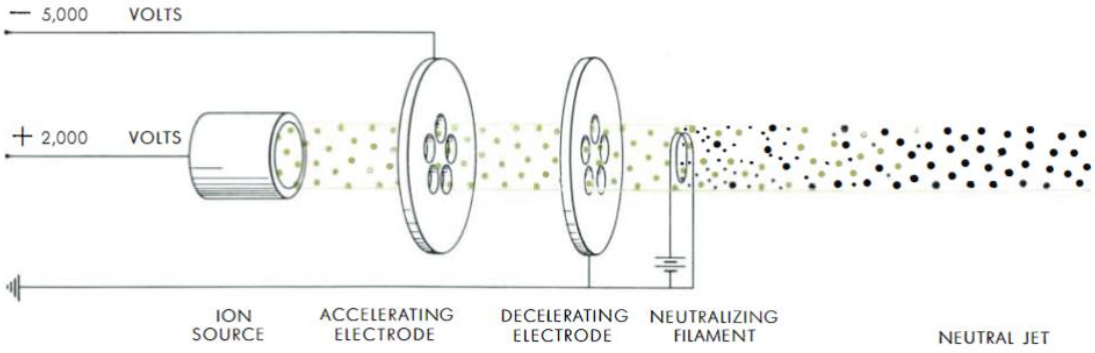

Figure 1-6 - Electrostatic engine diagram [12]

Figure 1.6 shows a diagram of an Electrostatic Engine. These engines work by accelerating a beam of positive ions using an electrostatic field [12]. Compared to chemical engines, the Electrostatic engine can accelerate these ions quicker than a chemical engine is able to expel fuel out of its nozzle [12].

Another less common method of propulsion is the use of a Nuclear Heat Transfer Rocket Engine. This engine creates power through heating up gases through nuclear fission of a nuclear material like Uranium [14]. Because of the use of highly reactive nuclear materials in the process, a Nuclear Heat Transfer Engine can produce an extreme amount of energy levels that chemical propellants cannot reach [14]. The only drawbacks about using Nuclear as a fuel source is that the high operating temperatures as well as the shear amount of energy produced by the system can cause structural integrity issues for the system [14]. Overall, an analysis of propulsion methods will be beneficial to the effectiveness of the system.

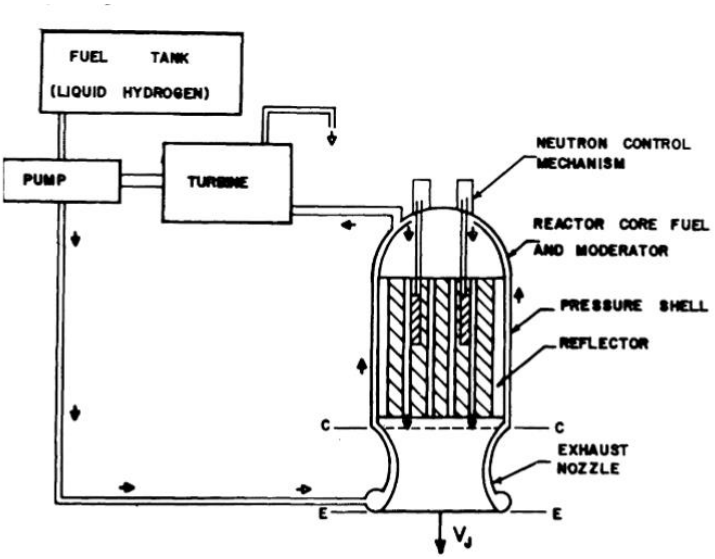

Figure 1-7 - Layout of nuclear heat transfer engine [14]

1.2.5 LIDAR and Imaging Sensing Methods

An imaging method will be of importance for a debris collection spacecraft. This will allow for the crew to spot potential debris that cannot be visually spotted by the human eye. While LIDAR is mainly used in the topological and geographical sense, its ability to measure distance through the timing of pulse travel allows for quick object detection [16]. NASA launched the Geoscience Laser Altimeter System (GLAS) on the IceSAT which is a LIDAR instrument that made observation of Earth possible from an orbiting satellite [16]. More specifically, GLAS was able to provide details on the height of atmospheric aerosol layers from space [16]. Although the GLAS LIDAR system was used to create images of Earth's atmosphere, LIDAR can be used in the scope of this project for object detection.

Figure 1-8 - GLAS LIDAR system [17]

While LIDAR could be an effective method of sensors for debris, there are also ground based (earth) methods that could be just as effective. The High Frequency Physics and Radar Techniques of the Fraunhofer Society developed the Tracking and Imaging Radar (TIRA) system that is capable of detecting objects in space. The big difference between TIRA and LIDAR systems is that the TIRA uses a Monopulse radar system [30]. While LIDAR is more accurate due to the use of a laser pulse rather than a radio wave, the use of a laser also means that the range is not as long as a radio wave from a radar system. The use of laser in a LIDAR system also means that LIDAR could also be sensitive to any low visibility conditions on the ground. Here, the TIRA can shine. While TIRA is not as accurate as a space-based LIDAR system, it can however be more dependable as well as farther ranged. TIRA can detect objects down to 2 cm large at around 1000 km range [30]. This means that this radar is more than capable of detecting objects in the ISS orbit and potentially even farther away if needed. As well as detection capabilities, the TIRA is also capable of tracking objects that it detects. In the subsystem requirement sections of the design, this project will go further into the decision on the detection system it will use to aid the completion of the system requirements.

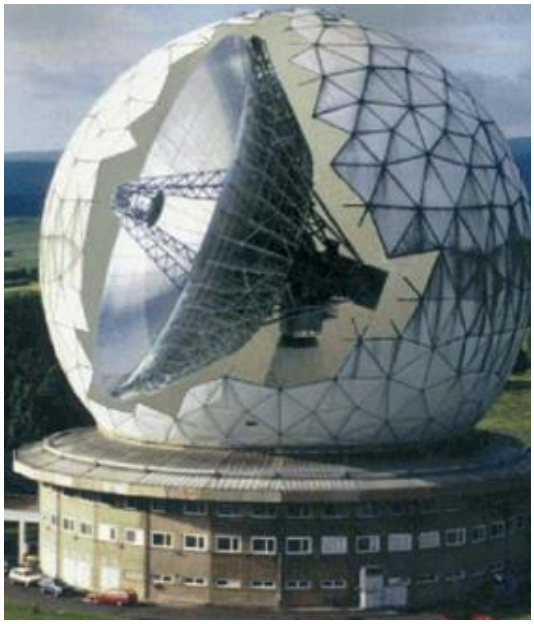

Figure 1-9 - TIRA Radar System (Dome Cutout for Visibility) [30]

1.3 Project Proposal

This project's objective is to go over the conceptual design of an object removal drone for the ISS. The spacecraft will look to collect any debris in the orbital path of the ISS that can cause potential damage from collision. Preventing the ISS from collision with orbital debris can reduce the financial costs of fixing damage caused by debris. The overarching goal of the project is to perform a complete system level design regarding different choices of propulsion methods, object detention sensors, as well as Module design that can allow for an efficient system.

1.3.1 Project Methodology

The methodology of this project will first entail studying the past designs of spacecrafts and their individual modules. This will help with making efficient use of space inside different spacecraft modules for the project. Analysis of available methods of propulsion like electronic, chemical, and nuclear methods will be needed to ensure the best outcome for the project. Propulsion efficiency values will need to be analyzed as well as thrust and engine ISP values to minimize fuel usage for this project. For object debris detection, past designs of LIDAR sensors as well as other detection methods will need to be studied as well. Any object detection laser installed onto the spacecraft will need to be ensured to have sufficient range to detect debris too far away for the human eye. Mechanically speaking, a closing and opening Iris will need to be designed for the debris collection. This will entail the use of Computer Aided Design software to reveal the mechanical workings of the system.

2 System Level Requirements

This chapter will discuss the overarching conceptual requirements of the project. Ideally, the spacecraft will be able to detect potentially dangerous space debris and remove it from the path of the ISS. Payload requirements include the ability for the spacecraft to be able to store debris and have enough space for spacecraft critical instruments. Specific requirements will be discussed within this chapter through in-depth discussion of select subsystem levels in individual chapters.

2.1 Mission Objectives

The objective of this spacecraft is to provide the ISS with protection from space debris through collection and the use of object detection instrumentation. The U.S Space Surveillance Network (SSN) can track objects around the orbit of Earth. If an object is detected to be in the orbital path of the ISS, the spacecraft can then be launched to collect the debris. Ideally, the vehicle will be launched from a docking port in the ISS and will work with the Space Surveillance Network to track the orbital path of the debris to match speed and collect the debris. When closing in on the debris, on board object detection radar systems will give the spacecraft a more exact location of the debris for collection. When finished, the spacecraft will then return to the docking port on the ISS and standby.

2.2 Space Debris Population

A general idea of the location and sizes of space debris in space will give this project a general idea on where it would be best to execute. Different orbital altitudes result in varying densities of space debris and so data surrounding this topic will be helpful. Research done by Alessandro Rossi and Giovanni Valsecchi shows that there are different clusters of space debris depending on the orbital inclination degree and the semi-major axis as shown in figure []. It is worth noting that the ISS has a semi-major axis of 6370 km, which roughly puts it at around the same semi-major axis as a Sun-synchronous orbit. The SSN can track all major objects with diameters over ten centimeters and clusters of such debris are apparent in specific altitudes near the ISS where we want to operate our spacecraft.

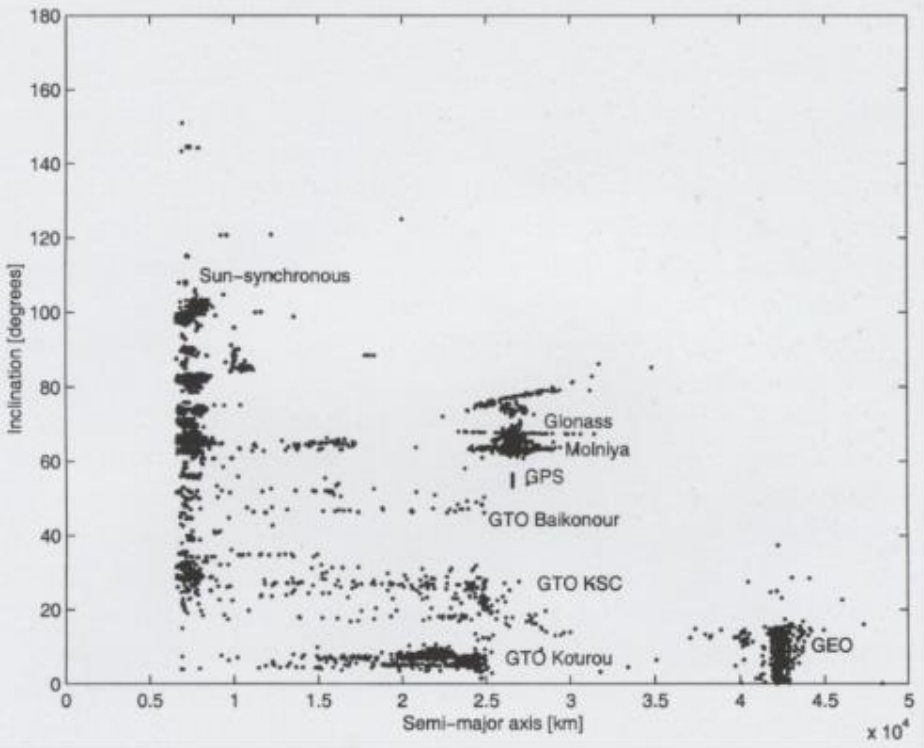

Figure 2-1 - Orbital debris clutter based on semi-major axis and inclination

2.3 System Specific Requirements

The chart below will map the overarching system requirements of the project's system.

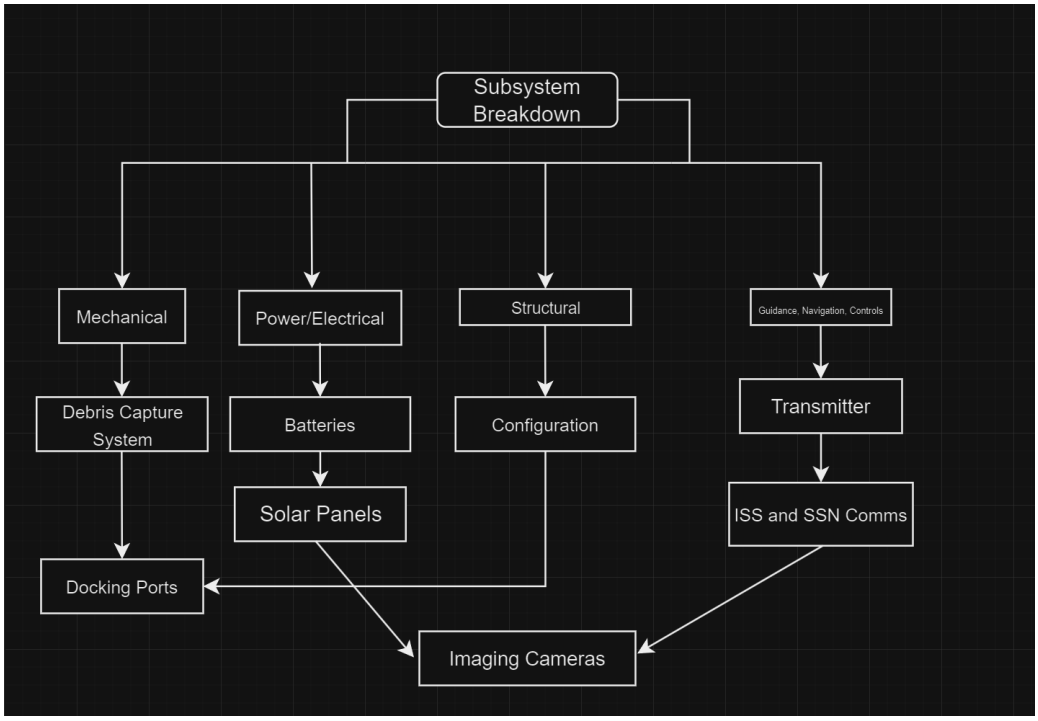

Figure 2-2 - Subsystem breakdown

2.3.1 Mechanical Requirements

The spacecraft will have to utilize a mechanical system for debris collection. Movement of the motorized system will need to be consistently repeatable as well as not physically interfere with other parts of the spacecraft. Here, a mechanical Iris open and close system would work very well as it would allow for collection of debris without using an external arm. The method of debris capture will be discussed in detail in this section as well, A docking system will also need to be able to dock on and off the ISS as well. Whichever docking system is used, whether it is a newly designed one or an existing one on the ISS, must be able to dock efficiently and allow for ISS access into the payload of the spacecraft.

2.3.2 Structural Requirements

The structure of this spacecraft will have to be able to hold the critical components of the spacecraft as well as the payload bay. The spacecraft frame will also have to be able to withstand the forces that are exerted onto the frame by propulsion as well. However, because the scope of

the project focuses on the spacecraft's functional ability as well as its hardware, the details of the structural subsystem will not be deeply analyzed.

2.3.3 Configuration Requirements

The layout of the spacecraft is vital to its overall system efficiency and performance. This section will include the layout of all instruments housed in the aircraft as well as the geometric design of the spacecraft. Placement of propulsion systems and potentially any solar panels for power requirements will be discussed in this section as well. Weight will also be another factor in the design of this spacecraft as this spacecraft cannot be too heavy to maximize propulsive efficiency.

2.3.4 Imaging and Detection Requirements

A camera will be required for the spacecraft to visualize its path towards an object when it is closing in. The camera on board will need to be able to give the spacecraft a visual of any debris that it is closing in on. Resolution and the zoom range of the camera will be a huge factor in the hardware selection as ideally this project needs a camera with sufficient resolution for the best clarity. Because of this, the potential use of optical lenses to

The chosen cameras for this system will also need to be mounted as well. Given the limited payload space and design constraints of such a project, design consideration must be made to make sure that any installed mount does not interfere with other mechanical aspects of the spacecraft.

Figure 2-3 - Nikon AF-S Teleconverter

For object detection, the literature review previously compared the benefits of both LIDAR systems and radar systems for this project. Although LIDAR is an effective tool to get accurate readings of distances of objects, the use of radar is more effective for its range and ease of implementation. The TIRA radar, as introduced previously, has two available radio bands for object detection: Ku band and L band [30]. While the integration of the Ku band is sufficient, the L band aspect of this radar not only allows for precise tracking, but high-resolution images. This is due to the nature of L bands being thin enough to penetrate through any low visibility conditions on Earth. L bands ability to penetrate through low visibility conditions make them a popular choice for communication satellites, such as the Iridium Next Satellite shown in figure 2.4. The Iridium Next Satellite will use K band radio waves for communication and will sit in GEO orbit. Because the ISS is in LEO, the use of the L band in the TIRA radar is more than sufficient for system requirements. Table 2.1 shows the different frequencies of the spectrum of radio waves as well as their respective wavelength and frequencies.

TIRA's powerful radar technology has allowed it to be consistently used by the European Space Agency for object detection in space [30]. As TIRA is already in service, the integration of TIRA and its communication with the ISS and ultimately the spacecraft will be much easier as the development of a new detection system will not be necessary. Ultimately, the variety of radar options that TIRA has to offer as well as the ease of integration makes TIRA a more attractive option. While LIDAR is more accurate, it is severely lacking in the range needed for system requirements and development an entirely new LIDAR system capable of having enough range will drive up costs for the project.

Table 2-1 - Radiowave Frequency Table [31]

Band	Approx. Range of Wavelength (cm)	Approx. Frequencies
UHF	100-10	300-3000 MHz
L	30-15	1-2 GHz
S	15-7.5	2-4 GHz
C	7.5-3.75	4-8 GHz
X	3.75-2.4	8-12 GHz
K	2.4-0.75	12-40 GHz
Q	0.75-0.6	40-50 GHz
V	0.6-0.4	50-80 GHz
W	0.4-0.3	80-90 GHz

Figure 2-4 - Iridium Next L Band Satellite

2.3.5 Guidance, Navigation, Communications

This subsystem section will cover the necessary equipment needed for communication from the spacecraft to the ISS as well as the SSN. The spacecraft will be required to keep continuous contact with the SSN to communicate the location of the space debris as well as the current trajectory it is on. Onboard communication systems and radios will be required to carry out communication between the spacecraft and the SSN/ISS. Allowing the spacecraft to work with the SSN will make for a much easier mission process as the spacecraft is able to tap into a very capable space detection network that cannot be installed on a smaller spacecraft.

Another necessity worth noting is the need for a high data rate transmitter. While there are many options as to what transmitter can be used on a satellite, the transmitter will ultimately need to be able to transmit data in an efficient manner without taking too much power to operate. A high data rate X band transmitter like the one in figure [19] can potentially be a great choice as its light weight and lack of power requirements makes for an efficient transmitter design.

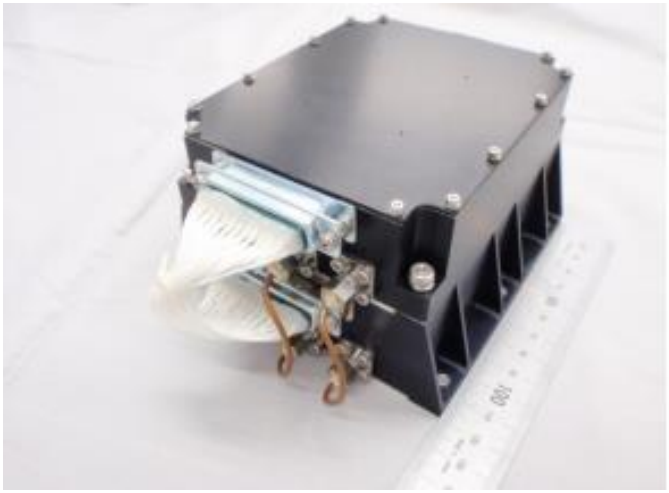

Figure 2-5 - High data rate X band transmitter [19]

2.3.6 Power Subsystem

A sufficient power system will be required to supply all on board instrumentation. While a onboard battery is a simple and efficient choice at supplying power, there can be other ways to provide additional power to the spacecraft should it be needed. The power subsystem section can also be potentially dependent on the propulsion subsystem as well as if the choice of propulsion is electric, the power system will have to be able to supply the propulsion power requirements as well. This subsection will go into detail about different choices of potential power sources and follow through on a selection of a specific power source.

2.3.7 Propulsion Subsystem

Different propulsion methods will be analyzed for the scope of this project as well. This project will weigh several benefits and drawbacks of different propulsion methods and will determine the best option for the mission objective. Fuel/power requirements will need to be calculated to ensure that the power needed to operate such chosen propulsion methods is sufficient to keep the spacecraft functional.

2.3.8 Concept of Operation

This section will detail the operation of a typical life cycle mission of the entire system. To begin, the spacecraft will be docked at the ISS and will use its comms to communicate with the ISS on any potential debris in the way. The debris will be spotted at a safe distance via radars onboard the ISS or via a space observation radar on Earth. After detection, only then will the spacecraft jettison from onboard the ISS and use its thrusters to maneuver away from the ISS and perform an orbital transfer towards the path of the debris. It will then capture the debris in question and then travel back towards the ISS to redock.

3 Mechanical Requirements

Mechanical Requirements will cover all topics that involve any moving parts of the spacecraft. Any chosen and designed mechanical systems on board the spacecraft will also be detailed in this section. Different debris collection designs and **techniques** will be discussed here as well as the integration of this spacecraft through the ISS through a docking system.

3.1 Debris Collection Methods

This subsection will discuss past designs of capture methods used by other satellites and spacecraft. Ultimately, this project will draw design features from multiple past projects to efficiently create one that suits this project's needs.

3.1.1 Magnetic Capture System

Astroscale's ELSA-D magnetic capture system is a project of interest as it features the ability for a satellite to dock onto another satellite magnetically [21]. This is highly beneficial for mechanical capture as a magnetic system means the ability to capture without a precise arm mechanism needing to grab an object and instead can capture an object just by being within the vicinity. However, there are also drawbacks to a magnetic capture design as this design would require the client that is being captured to have its own magnetic reaction plate [21]. One more thing worthy of noting here with the ELSA-D system is that this could also be implemented not only as a form of debris capture, but also a form of docking for the entire spacecraft. This will be further discussed in the configuration section.

Figure 3-1 - ELSA-D Magnetic Dock Capture System [21]

3.1.2 Tether Net Capture System

A tether net capture system is another viable solution to capturing debris. This method involves approaching the object and using a method of target capture through wrapping and closing the target [22]. Although at surface level it may seem like a simple design method of capturing, the dynamics of the entire process are very complex. This subsection will cover the different design elements of a tether net system.

3.1.2.1 Net Capture System

The tether net system involves a multi-step system that also involves the use of a casting tether as well as another collector module which in our case is the spacecraft itself. The spacecraft will open its own collection mouth that will spit out a tether and a net that will wrap itself around an object. A motor will also be connected to the tether and will wind it into the spacecraft for collection. This process is modeled in figure [22]. Additional thrusting will be needed to align the spacecraft more accurately into the axis of the target.

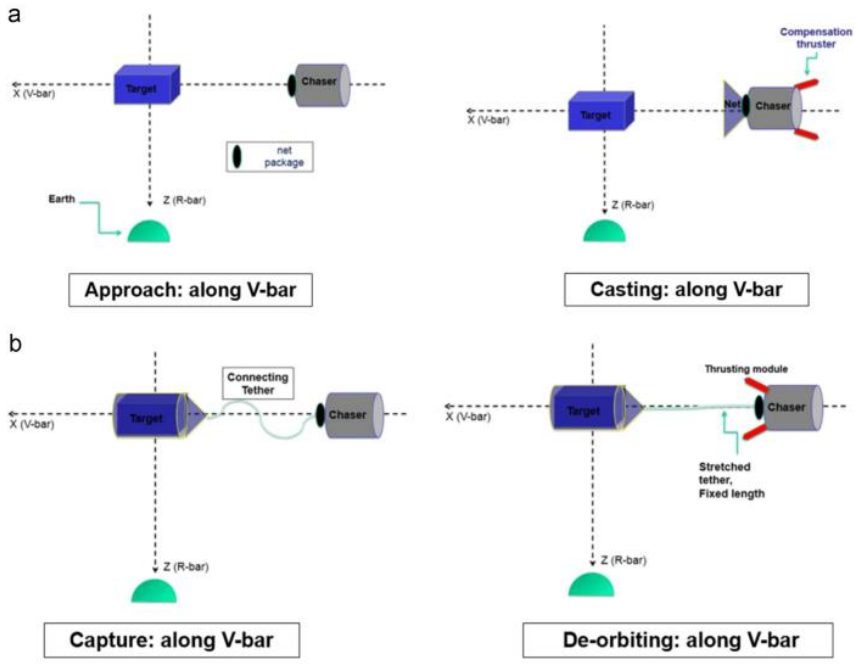

Figure 3-2 - Net capture system [22]

3.1.2.2 Modeling Dynamics and Capture Net Design

For a physical system like the tether net capture system, the forces of the casting net and the tug should be modeled, and the net material properties should be accounted for as well. As Ricardo Benvenuto's paper describes, the tension can be modeled through the equation

$$\boldsymbol{T_{ij}} = \left[-k_{ij}\left(\left|\boldsymbol{R_{ij}}\right| - l_{nom}\right) - d_{ij}\left(\boldsymbol{V_{ij}}\boldsymbol{R_{ij}}\right)\right]\boldsymbol{R_{ij}} \qquad if\left|\boldsymbol{R_{ij}}\right| > l_{nom} \quad [22] \qquad (3.1)$$

$$\boldsymbol{T_{ij}} = 0 \qquad if\left|\boldsymbol{R_{ij}}\right| \leq l_{nom} \quad [22] \qquad (3.2)$$

$$k_{ij} = \frac{EA}{l_{nom}} \quad [22] \qquad (3.3)$$

where $\boldsymbol{T_{ij}}$ represents the tension of the tether string, l_{nom} is the nominal length of the tether rope, k_{ij} is the axial stiffness equation, and $\boldsymbol{R_{ij}}$ and $\boldsymbol{V_{ij}}$ are the velocities and positions of the mass in question [22].

The d_{ij} term in equation (3.4) represents the damping of the tether with respect to the damping ratio ζ, angular velocity, and m_{ij} which represents the specific point mass between two points on the discretization of the net. An example of the discretization can be seen in figure

$$d_{ij} = 2\zeta w_{ij} m_{ij} \quad [22] \tag{3.4}$$

Now that the equation for tension is stated, Newton's Second Law can be utilized to form the equation of motion of the net.

$$m_i \frac{d^2 \boldsymbol{R_i}}{dt^2} = \boldsymbol{F_{GI}} + \sum_{j=-1,1} \boldsymbol{T_{ij}} + \boldsymbol{F_{ext}} \quad [22] \tag{3.5}$$

where $\boldsymbol{F_{ext}}$ is the external forces from perturbations, and $\boldsymbol{F_{GI}}$ is the gravitational force [22]. The summation inside equation (3.5) will represent the number of masses [22].

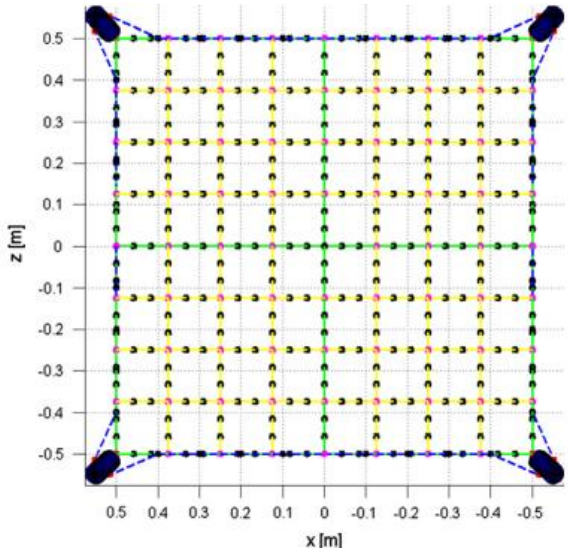

Figure 3-3 - Sample discretization of a 1 by 1 meter net [22]

After this, the dynamics of the full deployment can be modeled. Benvenuto's research executes a simulation of a full closing mechanism with an object rotating at five degrees per second and while using a planar net design compared to a pyramidal net closing design [22]. Figure [3.4] and [3.5] show the dynamical models regarding both net designs. One note is that the planar net used is a 30 x 30-meter size net for larger objects while the pyramidal is set at 1 x 1 meters. This is also noted in the target size simulation parameters inside figures 3.4 and 3.5. Tables 3-1 and 3-2 below reveal the full simulation parameters.

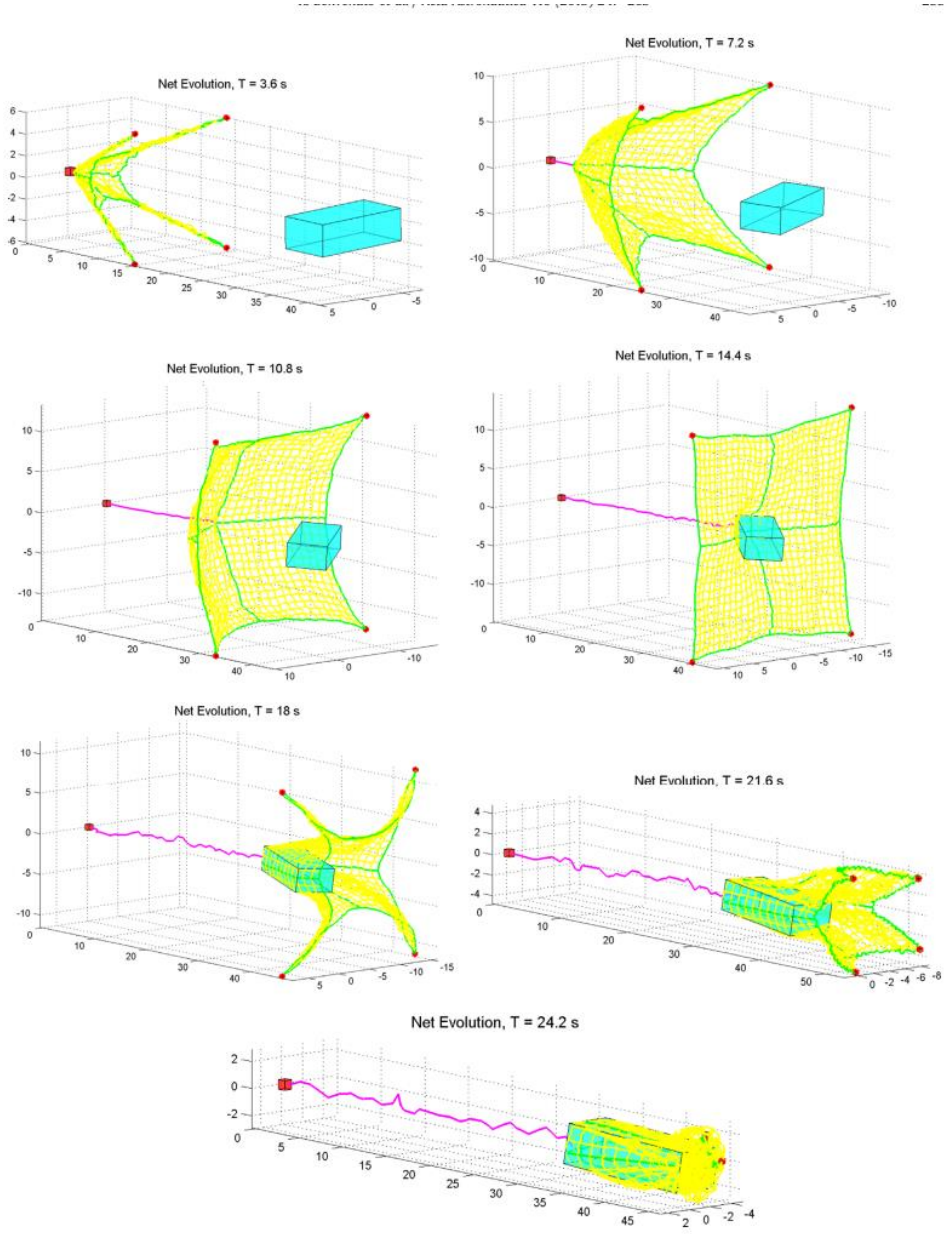

Figure 3-4 - Planar net dynamical capture simulation [22]

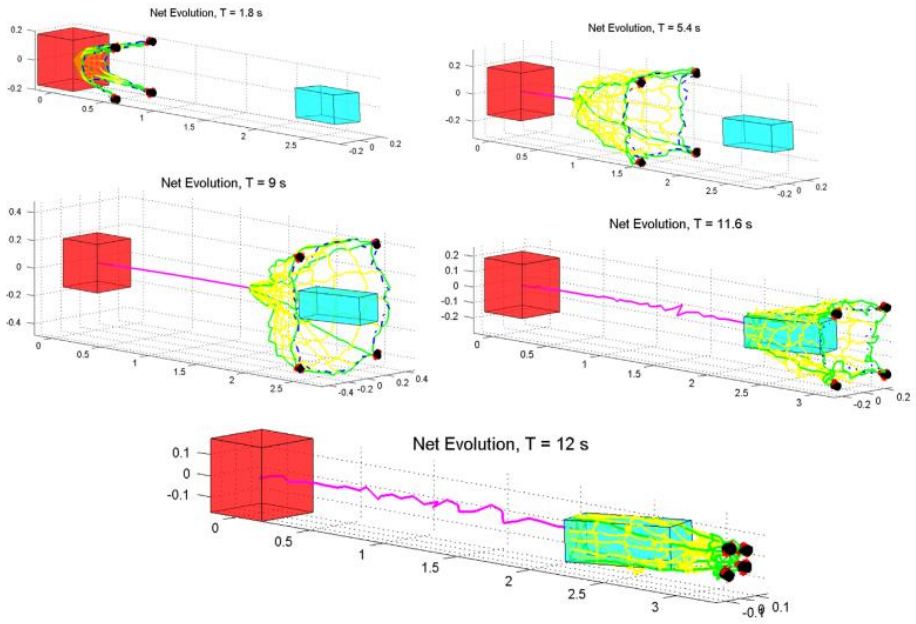

Figure 3-5 - Pyramidal net dynamical capture simulation [22]

Table 3-1 - Planar net simulation parameters [22]

Planar net parameters.

Type	Planar (13107 DOF)
Size (m)	30×30
Mesh (m)	1×1
Mass (kg)	4.269
Bullet Initial Impulse (N)	3.47
Closing time (s)	10
Target size (m)	$5 \times 3 \times 10$
Target angular velocity (deg/s)	5

Table 3-2 - Pyramidal net simulation parameters [22]

Pyramidal net parameters.

Type	3D-pyramidal (2859 DOF)
Size (m)	1×1
Mesh (m)	0.25×0.17
Mass (kg)	0.716
Bullet Initial Impulse (N)	0.49
Closing time (s)	0.3
Target size (m)	$0.2 \times 0.2 \times 0.6$
Target angular velocity (deg/s)	3

Here the simulation clearly shows the results of using both the planar net and the pyramidal net design. With a planar net design, the large net is required to capture a larger object while with the pyramidal design, the caving design of the net allows for better capture of smaller objects [22]. For the application of the project, it would be beneficial to include both uses of a larger and smaller net design for debris of varying sizes. Furthermore, the four-way plane interlace design also contributes to a better lock and capture of debris as the net closes in on all four corners of itself [22].

4 Propulsion System Selection

The selection of propulsion systems was done by taking into consideration the different available propulsion methods as well as the integration of the entire system into the configuration layout. Along with configuration, the amount of provided thrust from a propulsion system as well as the energy needed to power the propulsion system will also be considered here. Ideally, a combination of a stronger source of thrust will be used as the main propulsion source for this application while a smaller source of thrust will be utilized to make finer adjustments when aligning the spacecraft. This section will dive into different engines that can potentially be used for this project.

4.1 Main Propulsion System

The main propulsion system of the spacecraft will be the most powerful thrusters on board. These thrusters are system critical and will be responsible for moving the spacecraft to debris locations and to the ISS. Ideally, the selected engines on board will need to be able to start and stop multiple times to allow for accurate placement of the spacecraft during the mission process. Burn time will be a factor as well as the engine will need enough burn time to complete its mission as well. Integration of the engine into the overall configuration of the project will also need to be factored into selection as well.

A secondary engine will also be necessary to make the finer adjustments needed to locate the spacecraft more precisely with respect to the capture of debris. For this, an engine with smaller amounts of thrust is preferred so that the position of the spacecraft can be finely adjusted. Placement of this thruster will also need to be strategically placed to maximize the fuel efficiency of the spacecraft.

4.1.1 Main Engine Selection

For this section of the design, there are many differing selections of engines, each with their own benefits and drawbacks. Cryogenic engines can provide high amounts of thrust while also being light for the thrust it is able to produce. However, these engines do need special care due to the extremely low temperatures of the fuel and oxidizer. This project will investigate the Aerodyne J2 as a potential engine selection for this spacecraft. Aerodyne’s J2 was used in the Saturn V rocket’s fourth stage and is designed to be reignited while also being able to produce a significant amount of thrust.

Another form of propulsion that can be considered is a hypergolic rocket which is less powerful but will be less difficult to maintain and operate than cryogenic engines. SpaceX’s Draco engine is a potential selection here like the J2, this engine can also be reignited. However,

one benefit that stands out from the J2 engine is that Draco, like other hypergolic propellants, does not need to be ignited for combustion. The Draco is also capable of repeatedly reducing its thrust levels as this thruster was originally designed for propulsion landings [26].

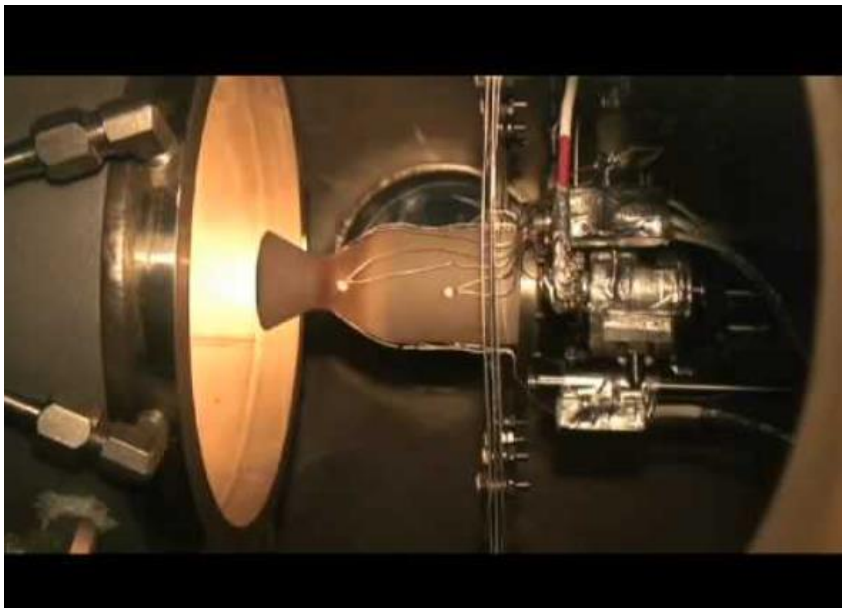

Figure 4-1 - SpaceX Draco thruster [23]

Table 4-1 - Engine catalog with specifications regarding thrust, size, and mass

Engine	**Max Thrust**	**Isp**	**Dry Mass**	**Diameter**	**Length**	**Propellant**	**Burn Time**
J2	486.2 kN (at SL)	4.13 km/s	1438 kg	2 meters	3.38 meters	LOX, LH2	475 S
Draco	71 kN (at SL)	2.9 km/s	Undisclosed	20 cm (Exit)	≅1 m	NTO, MMH	354 S
NSTAR Thruster	92.4 mN	30.57 km/s	27.53 kg	41 cm	≅50 cm	Xenon	>8000 hours

4.1.2 Secondary Engine Discussion

One possible selection here could be the use of NASA's NSTAR Ion thruster. The NSTAR thruster is designed by NASA and best suited for spacecrafts in need of high degree delta v maneuverability [24]. Although Ion thrusters do not provide the levels of thrust compared with more conventional propulsion methods, this is not necessary as these engines are only used for micro adjustments. Figure 4.2 also shows the dimensions of the NSTAR thruster. Configuration wise, the NSTAR thruster does not take up much space. This will help with the configuration of the spacecraft as there is more space to fit other components. Figure 4.3 shows the different available throttle levels of the NSTAR engine alongside the voltage and amperage requirements of the thruster. Later sections of this project will discuss the power requirements of all the components in this spacecraft.

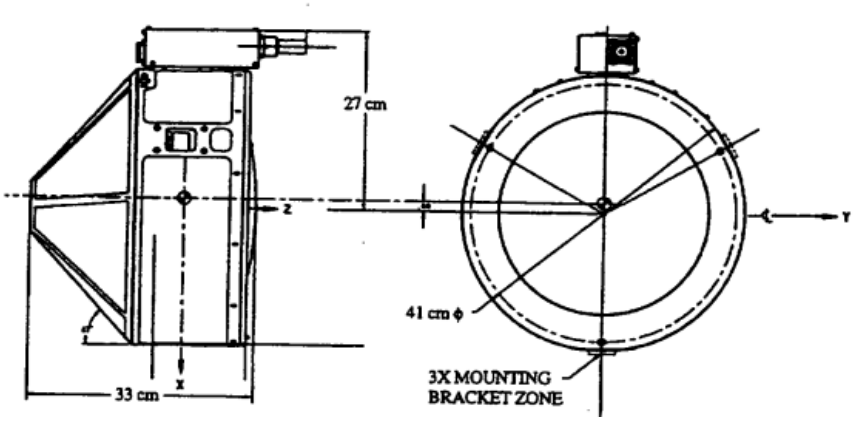

Figure 4-2 - NSTAR thruster dimensions [25]

Table 4-2 - NSTAR throttle levels and requirements [24]

NSTAR Throttle Level	Mission Throttle Level	PPU Input Power (kW)	Engine Input Power (kW)	Calculated Thrust (mN)	Main Flow Rate (sccm)	Cathode Flow Rate (sccm)	Neutralizer Flow Rate (sccm)	Specific Impulse (s)	Total Efficiency
15	111	2.52	2.29	92.4	23.43	3.70	3.59	3120	0.618
14	104	2.38	2.17	87.6	22.19	3.35	3.25	3157	0.624
13	97	2.25	2.06	82.9	20.95	3.06	2.97	3185	0.630
12	90	2.11	1.94	78.2	19.86	2.89	2.80	3174	0.628
11	83	1.98	1.82	73.4	18.51	2.72	2.64	3189	0.631
10	76	1.84	1.70	68.2	17.22	2.56	2.48	3177	0.626
9	69	1.70	1.57	63.0	15.98	2.47	2.39	3136	0.618
8	62	1.56	1.44	57.8	14.41	2.47	2.39	3109	0.611
7	55	1.44	1.33	52.5	12.90	2.47	2.39	3067	0.596
6	48	1.32	1.21	47.7	11.33	2.47	2.39	3058	0.590
5	41	1.19	1.09	42.5	9.82	2.47	2.39	3002	0.574
4	34	1.06	0.97	37.2	8.30	2.47	2.39	2935	0.554
3	27	0.93	0.85	32.0	6.85	2.47	2.39	2836	0.527
2	20	0.81	0.74	27.4	5.77	2.47	2.39	2671	0.487
1	13	0.67	0.60	24.5	5.82	2.47	2.39	2376	0.472
0	6	0.53	0.47	20.6	5.98	2.47	2.39	1972	0.420

4.1.3 Engine Suite Selection

The overall selection suite for the engines will involve the use of 6 draco thrusters on two sides of the spacecraft for a total of twelve. Use of a secondary engine was initially considered although, however, it was concluded that the use of Draco thrusters for both primary and secondary duties would be most efficient. The NSTAR thruster is a thruster that provides high power output efficiency as well as prolonged amounts of thrust. While the NSTAR thruster could make a very good choice for secondary positioning thruster due to its low power output as shown in table 4-2, the mission design for this project does not ultimately reap the benefits of an Ion thruster. The mission profile is relatively short and does not involve multiple changes of orbital paths. Because of this, it was thought best that the Draco thruster be the main source of thruster, as well as the secondary positioning thruster.

5 Power Requirements

The power requirement section of this spacecraft will be selected based upon previous missions as well as this project's requirements. All critical components such as communications, camera, and mechanical equipment onboard will require adequate power. This spacecraft will also need to be able to generate enough power to keep the spacecraft in service for extended periods of time. On top of the need to generate enough power to keep the spacecraft in service, the discussion of energy storage will also be analyzed as well and the different approaches that are available for the project.

5.1 Power Selection Discussion

While there are many potential power sources for this project, every source has its own benefits and drawbacks that must be analyzed for the project requirements. This section aims to analyze the different choices of power for this project. Nuclear power sources will be discussed here as well as solar power sources and battery types.

The first power source that will be discussed is the use of nuclear power sources. Nuclear power can be considered here as using would mean a more consistent source of power when compared to using solar power. Nuclear power would be used in the form of a Radioisotope Thermoelectric Generator (RTG) and this system would work through by decaying Plutonium for heat. Because Plutonium takes a long time to decay, this makes RTG a good source of energy for extended space missions where sunlight is inconsistent. The Snap-19 RTG is shown in Figure 5-1 shows the Radioisotope fuel capsule along with its Thermoelectric elements that convert the heat from the decay into usable electricity [27].

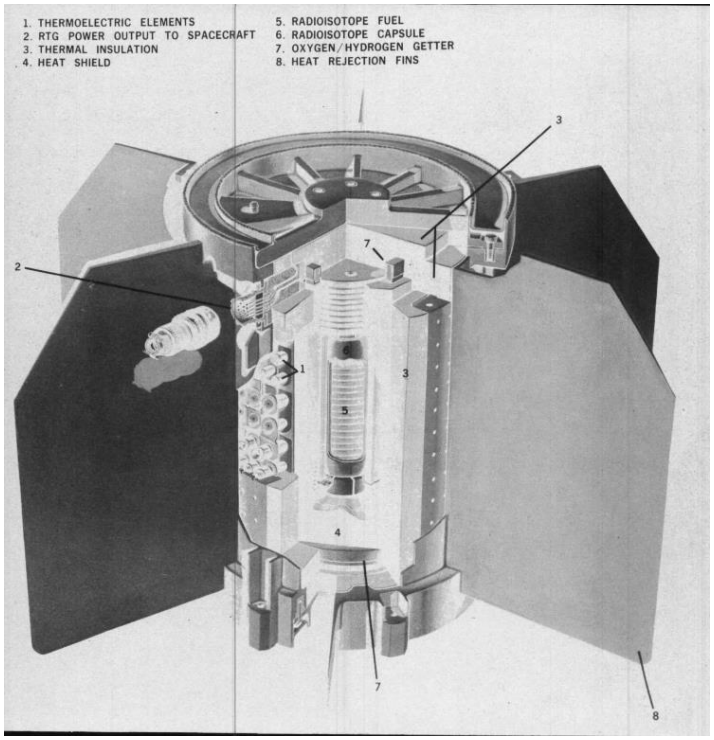

Figure 5-1 - RTG Diagram

However, the use of Nuclear Power in an application such as this project has its drawbacks as well. RTG's are inherently dangerous as they include a highly radioactive component in the Radioisotope capsules/fuel source. Equipment could also be potentially damaged as the cameras on board the spacecraft could be damaged in the event of a nuclear meltdown or accident. Heat also presents itself as a potential danger as the decay of Radioisotopes is not efficient, and thus critical components must be shielded from excessive heat.

A more common power source that could be viable for this spacecraft is the use of Solar power through photovoltaic solar panels. Choosing photovoltaic solar as a power source will also require the necessity of an energy storage method for storing power in case of periods of high-power demands or eclipses [29]. Benefits of choosing a more traditional solar source are that the system is much simpler to build and operate. Constructing the solar arrays is simple as all it takes is to build arrays in a series [28]. Because of this, it is easy to physically scale the design of such an array to the project's power requirements.

Although nuclear power RTG's can provide consistent power that does not require a source of sunlight to generate, there are too many drawbacks that far outweigh the benefits it can bring to the spacecraft. The potential of nuclear fallout onboard the spacecraft as well as the high costs of implementing nuclear power sources are also a negative that cannot be ignored. Finally, RTG's are popular for deep space missions because of their ability to produce consistent power over long periods of time. However, because our spacecraft only has the objective of removing

debris in the orbital path of the ISS, the benefits of RTG's cannot be reaped. Therefore, photovoltaic solar power will be the choice of power for this spacecraft.

5.2 Energy Storage Discussion

This section will discuss all the calculations needed for energy storage for the spacecraft. The choice of solar array material as well as efficiency values will be discussed. Included in the calculations will be the solar array power output as the solar array sizing for the spacecraft. Finally, the end-of-life power production capabilities of the solar array will be analyzed in this section as well. All the calculations for energy storage will be completed using the Space Mission and Design handbook (SMAD) [29].

Before going on the discussion of energy storage, we must consider the power requirements of the system as well as the availability of sunlight as well as the time spent in eclipse. This way, the information and variables needed to calculate energy storage parameters and solar array sizing values is possible. For an estimate of the power that includes headroom, the spacecraft power subsystem will need to generate 2000 watts for the entirety of the system. For the power transfer from the solar array to the battery loads, the system will use direct transfer, meaning that a power converter is not needed between the array and the loads. SMAD references the path efficiencies of these values for eclipse and daylight to be 0.65 and 0.85 respectively. Now for the power requirements, the spacecraft will not have varying power requirements when it is in eclipse or sunlight, the power requirements will be consistent for all our calculations. Finally, because the orbital period of the ISS is 90 minutes, this means that the ISS will experience eclipse and daylight at 45-minute periods each, thus six hours of sunlight and daylight per orbital period. The spacecraft will experience the same cycle for the further discussed calculations

With choosing photovoltaic solar power for the spacecraft, the solar array area must also be calculated. This is done through first calculating the amount of power the solar array needs to generate during periods with ample sunlight. The equation for solar array power is represented through:

$$P_{sa} = \frac{\left(\frac{P_e T_e}{X_e} + \frac{P_d T_d}{X_d}\right)}{T_d} \qquad [29] \tag{5.1}$$

$$P_{sa} = \frac{\frac{(2000W \cdot 6\ hr)}{0.65} + \frac{(2000W \cdot 6\ hr)}{0.85}}{6\ hr} = 6153.84\ W$$

where P_{sa} is the total solar array power, P_e and P_d is the power requirements during eclipse and daylight respectively, X_e and X_d are path efficiencies of the solar array's relationship with the battery and the load, and T_e and T_d is the length of the eclipse and daylight respectively.

After obtaining the total solar array power of the system, the estimated power output P_o needs to be calculated. The calculations for the total solar array power are dependent on the type of Photovoltaic solar cell that is chosen for the project. A variety of choices for Photovoltaic solar cells are available and are outlined in the table below.

Table 5-1 - Performance Comparison for Photovoltaic Cells [29]

Cell Type	**Silicon (Si)**	**Thin Film Amorphous Si**	**Gallium Arsenide**	**Indium Phosphide**	**Triple Junction Gallium**
Planar Cell Theoretical Efficiency	29%	12%	23.5%	22.8%	40+%
Achieved Efficiency:	22%	8%	18.5%	18%	30%
Equivalent Time in GEO for 15% degradation - 1 MeV electrons - 10 MeV protons	10 yr 4 yr	10 yr 4 yr	33 yr 6 yr	155 yr 89 yr	33 yr 6 yr

The chosen material for Solar Cell for this project will be the use of Triple Junction Gallium Arsenide (GaA) cells. Because the ISS is at LEO and above the Earth's protective ozone layer, it is exposed to potential radiation damage from the Sun. GaA cells are protective against radiation when compared to the other options on Table 5-1 [29]. Because of the added radiation protection GaA cells offer, it is also the costliest option. However, radiation protection is non-negotiable for the design of this project and thus will be necessary for the completion of the power system design.

Now with the chosen choice of materials for the Solar Cell, we are then able to proceed with the calculations for the estimated power output P_o. According to the SMAD handbook, the estimated power output of a Triple Junction GaA cell can be represented by the equation

$$P_o = 0.28 \cdot 1{,}368 \frac{W}{m^2} \quad [29] \tag{5.2}$$

$$P_o = 383\ w/m^2 \tag{5.2}$$

After calculating for the estimated power output, the calculations for the power availability per solar array needs to be calculated. Although solar arrays have their calculated efficiencies, the actual solar array will degrade from installation, high temperatures, as well as cell shadowing [29]. The SMAD handbook overviews the different aspects of solar array degradation and estimates that the nominal Inherent Degradation value I_d is around 0.72 [29]. This value of Inherent Degradation will be used to calculate the beginning of life power capabilities (P_{BOL}) of the solar array. Beginning of life power capability can be represented as

$$P_{BOL} = P_o I_d \cos(\theta) \quad [29] \tag{5.3}$$

The value of θ here represents the Sun incidence angle in which the assumption is that a perpendicular ray of sunlight represents the maximum power for the solar array. This is known as Cosine Loss [29]. Estimating that the worst-case scenario sun angle to be 23.5 degrees, the equation then becomes

$$P_{BOL} = (383)(0.72)\cos(23.5°) \tag{5.3}$$

$$P_{BOL} = 252\ w/m^2 \tag{5.3}$$

Now that the beginning of life capabilities has been calculated, the end-of-life capabilities now need to be analyzed as well. The performance degradation of triple junction GaA cells is 0.5% per year [29] and such, the total degradation can be represented as

$$L_d = (1 - D)^L \quad [29] \tag{5.4}$$

$$L_d = (1 - 0.5)^5 = \ 0.03125 \tag{5.4}$$

where L is the satellite life in years, and D is the degradation per year. Ideally, the spacecraft would remain in service for 5 years at the ISS.

With the total degradation now calculated, the end-of-life performance can now be calculated as

$$P_{EOL} = P_{BOL} I_d \quad [29] \tag{5.5}$$

$$P_{EOL} = (252)(0.72) = 181.44 \ W/m^2 \tag{5.5}$$

With the end-of-life capabilities analyzed, the solar array area can finally be calculated as such. This is represented as

$$A_{sa} = \frac{P_{SA}}{P_{EOL}} \qquad [29] \tag{5.6}$$

$$A_{sa} = \frac{6153.84}{181.44} = 33.917 \ m^2 \tag{5.6}$$

This now concludes the calculations for solar array area. The value of 33.917 m^2 of solar area is a plausible solution as this would mean a solar panel of around 6 meters by 6 meters. This value is going to be integrated in the configuration section moving forward.

5.3 Battery Suite

As discussed in the previously, an energy storage method is needed for a photovoltaic solar source. The Space Mission Design and Analysis textbook will be extensively referenced here as it provides many battery options for power storage. A primary and secondary battery choice will be discussed, as this spacecraft will need a battery capable of storing high amounts of power and another that is capable of being recharged for high power situations and/or eclipses [29]. Table 5.1 shows a variety of common choices of primary batteries available to choose from as well applications that each specific battery is used for.

Table 5-2 - Primary Battery Selection Table [29]

Primary Battery Types	Specific Energy (WHr/kg)	Typical Application
Silver Zinc	60-130	High rate. Short life (minutes)
Lithium Thionyl Chloride	175-440	Medium rate, moderate life(<4 hours)
Lithium Sulfur Dioxide	130-350	Low/Medium rate, long life (days)
Lithium Carbon Monofluoride	500-800	Low rate, long life (months)
Thermal	30-60	High rate, very short life (minutes)

Because this mission is neither a deep space mission nor a mission requiring multiple stages that require long periods of time with power, the choice of the primary batter here will be Lithium Carbon Monofluoride. An LCM battery will provide a low discharge rate while lasting for months on end, allowing for the spacecraft to stay on mission and/or standby for extensive periods of time. Primary batteries will be the main source of power for this spacecraft, but it is important to note that these batteries cannot be charged [29]. Because these batteries cannot be charged, a secondary battery will be needed for the spacecraft to operate in eclipse conditions.

Like the choice of primary batteries, the SMAD guidebook offers a guide and catalog on the selection of secondary batteries. Although the secondary battery will have less energy density compared to the primary battery, the secondary battery is able to convert chemical energy into electrical energy and vice versa repeatedly [29]. The rechargeability of the secondary battery makes these batteries ideal for backup power or for periods where extensive power is needed [29]. The characteristics of some potential secondary battery options are shown in table 5-2 as well as the potential impacts and notable pointers of each battery type.

Table 5-3 - Secondary Battery Selection Table and Characteristics

Performance characteristics	**Ni-Cd**	**Ni-H_2**	**Li-Ion**	**System Impact**
Energy Density (W-hr/kg)	30	60	125	Mass saving and vehicle center of gravity
Energy Efficiency (%)	72	70	98	Reduction of charge power reduces solar panel mass and size
Thermal Power (1-10)	8	10	1	Reduction of radiators, heat pipes sizes
Self-Discharge (% per day)	1	10	0.3	Simple management at launch pad and more margin during transfer
Temperature Range (°C)	0 to 40	-20 to 30	10 to 25	Management at ambient and thermal control reqs
Memory Effect	Yes	Yes	No	No reconditioning management
Energy Gauge	No	Pressure	Voltage	Easier state of charge assessment
Trickle Charge	Yes	Yes	No	Balancing need prior to eclipse, Li-Ion typically requires cell equalization circuitry
Modularity	No	No	Yes	One Cell Design
Heritage	Yes	Yes	Yes	Risk Assessment, Continued Li-Ion LEO testing and missions establishing heritage.

Another piece of data that is worth mentioning from the SMAD textbook is the depth of discharge of the secondary batteries. With each cycle of charge, the batteries on board will slowly lose their maximum capacity. An increase of the depth of discharge percentage means a lower maximum capacity for the battery. As well as depth of discharge, the energy density of the battery also needs to be considered in the selection of a secondary battery.

Considering all the variables from table 5.2, the choice of the secondary battery for this spacecraft will be a Lithium-Ion battery. Although looking from a depth of discharge perspective makes this a less desirable choice, the high energy density of a Li-Ion battery makes it a more desirable choice for prolonged missions. Furthermore, Li-Ion batteries can be operated at a higher voltage when compared to Nickel Cadmium or hydrogen batteries [29]. This ultimately means that less cells are needed when compared to other battery choices of lower voltages.

5.3.1 Secondary Battery Sizing

For the last part of the battery calculations, the battery sizing will be calculated for. The battery sizing is dependent on the capacity equation, Battery capacity (C) can be represented as

$$C = \frac{(P_e T_e)}{(DOD \cdot N \cdot n)} \quad [29] \tag{5.7}$$

where P_e and T_e is the average eclipse load and the time of eclipse respectively. DOD represents the depth of discharge, N represents the number of batteries, and n represents the battery to load transmission efficiency [29]. The eclipse load as well as the time of eclipse was estimated for in equation (5.1) and therefore, we will be utilizing the same values for the battery capacity calculations. For Lithium-Ion batteries, the depth of discharge can be estimated at 30% and the transmission efficiency can be estimated to be around 90% [29]. Last of all, the number of batteries is up to design discretion and as a higher number of batteries will mean less individual capacity, while a lower number would require a higher capacity to compensate for the limited battery number. As such, this project will stick with three batteries. Plugging in all the values and we get that

$$C = \frac{(2000\ W \cdot 6\ hr)}{(0.3 \cdot 3 \cdot 0.9)} = 14{,}814\ W\ hr \tag{5.7}$$

While the 14,814-watt hour requirements may seem high at first glance, this is not beyond the possibility of implementation. Often, large Lithium-Ion batteries are created to power

homes off the grid, such as the ones in figure 5-2 [32]. Table 5-2 also shows some of the important specifications of the specific 14 kwh Lithium-Ion battery from BatteryEvo. Form factor wise, this battery is quite small relative to the power it is able to deliver, only coming in at 43.4 inches by 26.7 inches. This means that this battery can easily be stored within one of the cockpit compartments, in which we will go over in more detail in the configuration section of this project.

Figure 5-2 – BatteryEvo Lithium-Ion Battery [32]

Table 5-4 - BatteryEvo 14 kwh Li-Ion Specifications [32]

Charge Temperature Range	Discharge Temperature Range	Optimal Discharge Range	Storage Temperature Range	Weight	Depth	Width	Height
0° C - 55° C	-20° C - 55° C	15° C - 35 ° C	-5° C - 35° C	131.5 kg	11.2 cm	110 cm	67.8 cm

6 Configuration Design

The spacecraft will consist of two main sections: the cargo bay as well as the main section which houses the operators of the spacecraft. This section will detail the overall layout of the spacecraft equipment and instruments. Placement of camera imaging systems, power systems, propulsion systems, as well as the geometry of the spacecraft will be detailed out in this section, Previous and related mission configurations and designs will also be considered for inspiration into the process of completing the design of this spacecraft as well. The SolidWorks CAD will be utilized to show the layout of all the systems.

6.1 Discussion

There will be three total sections outlined for this spacecraft in total. This includes the nose cone, fuselage and cargo bay, as well as the docking port. All three of these sections will be discussed in their entirety in the upcoming sections. The spacecraft in total will be around 17 meters tall while the diameter of the main body will be 7 meters wide.

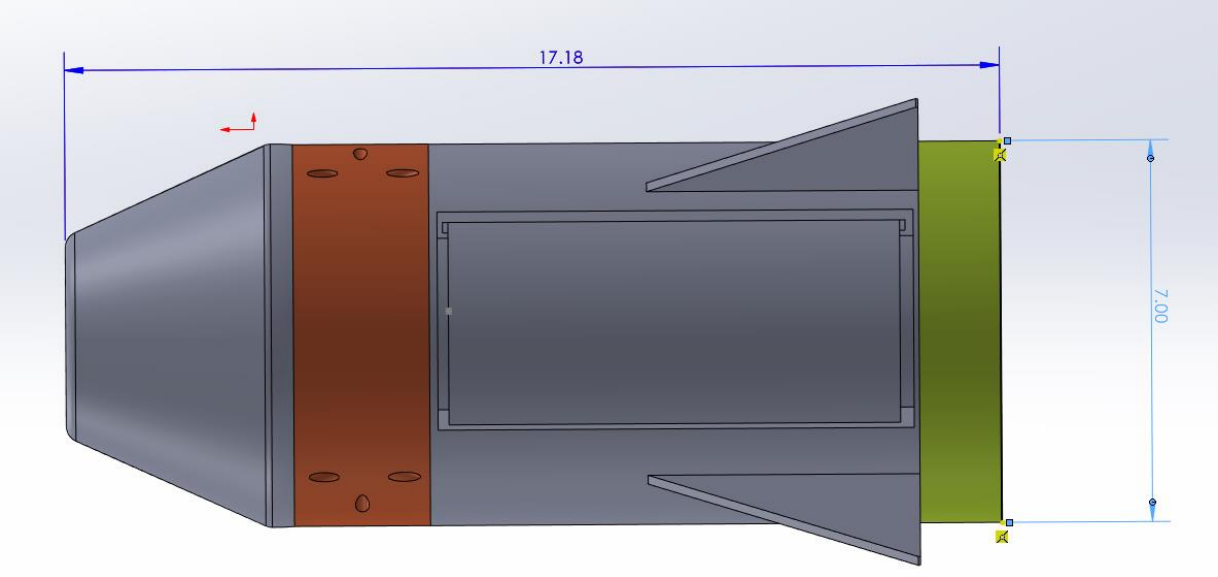

Figure 6-1- Overall configuration dimensions

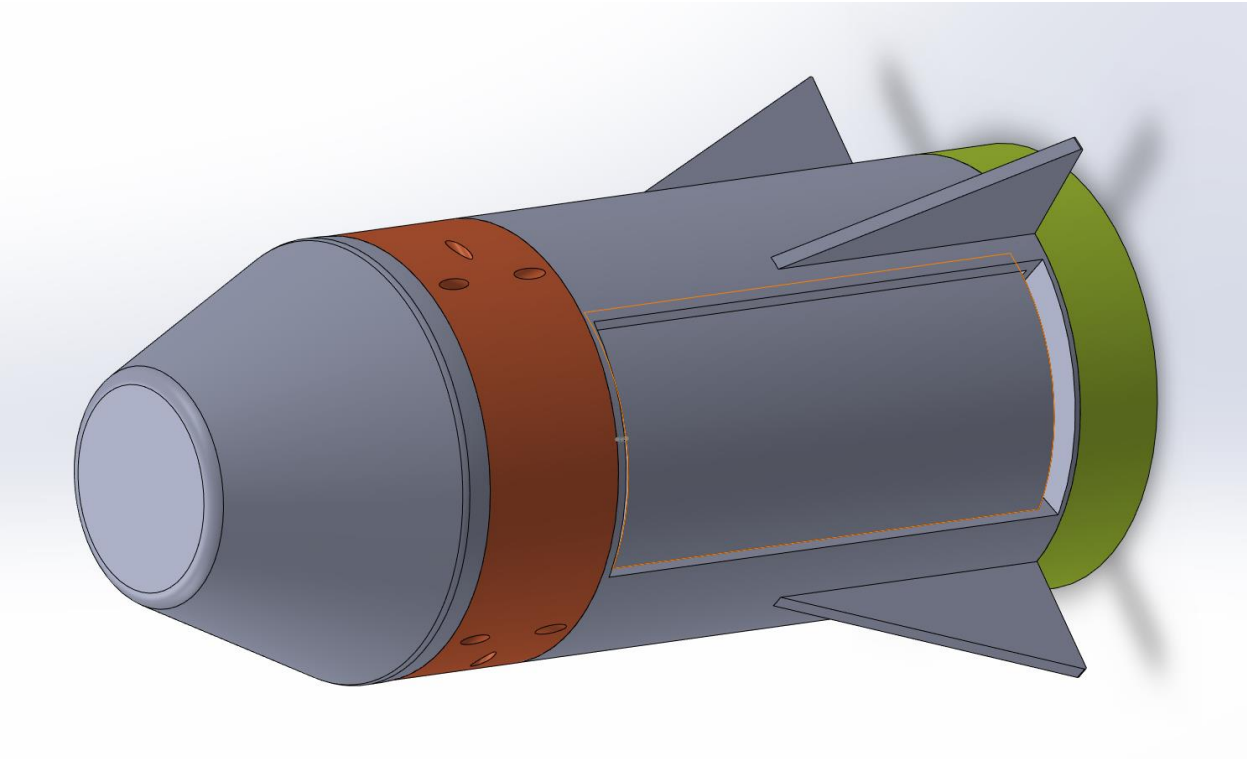

Figure 6-2 - Overall configuration with cargo bay closed (Iso View)

6.2 Cargo Hold Design

The cargo hold design will involve the overall configuration of the debris storage area and some of the system critical components. The net tether system discussed earlier will be stored in its own cargo section of the spacecraft. A sliding door mechanism will be used to open and close the storage hold. This allows for efficient opening and closing access into the payload for debris entry. When opening, the two doors will slide into a small slit storage area of the structure. Designing the payload door in this way allows for the door to operate without obstructing any external or internal parts. Figure 6-2 and 6-1 shows the closed configuration where the sliding door of the fuselage is not retracted.

Between the main cargo bay and the nose cone sits the space for fuel and thrusters. This space is marked in an orange color on the CAD models. Four groups of three cutouts are made on this area to show the mounting points of the Draco thruster that will be used for propulsion on this spacecraft. A total of twelve thrusters will be used for propulsion and maneuvering of the spacecraft. Fuel will be stored all around the thruster area in the o- ring shaped spacer so there is space in the middle to allow for access between the nose section and the cargo bay. This is shown in figure 6-3.

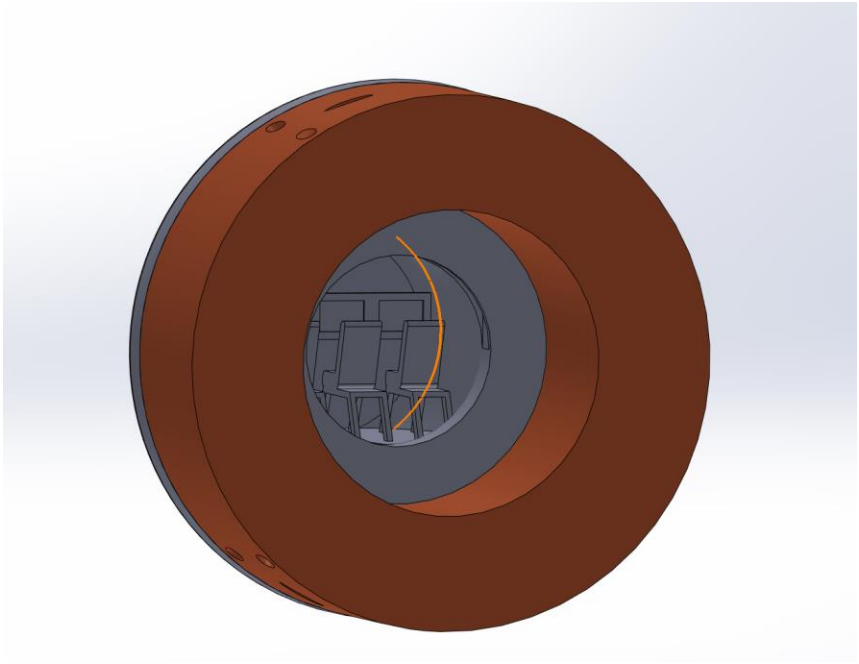

Figure 6-3 - Cutout of Nose Cone and Fuselage section looking into cockpit

As mentioned previously, this spacecraft will capture debris via a net tether system and pull debris in to store in its cargo bay. The sliding cargo bay door will open and go into the door slit while the capture net will be pushed out as shown in figure 6-4.

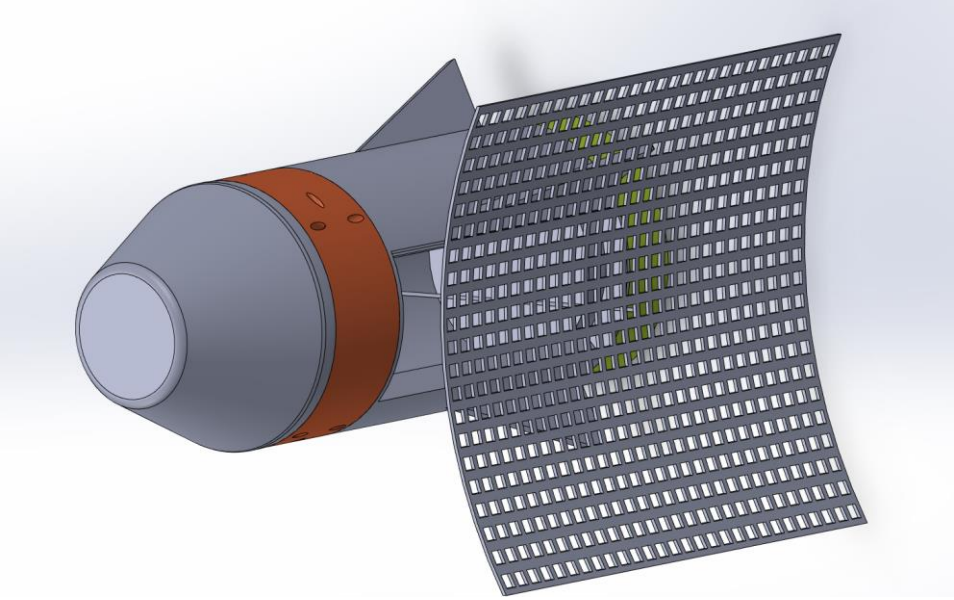

Figure 6-4 - Capture net implementation (iso view)

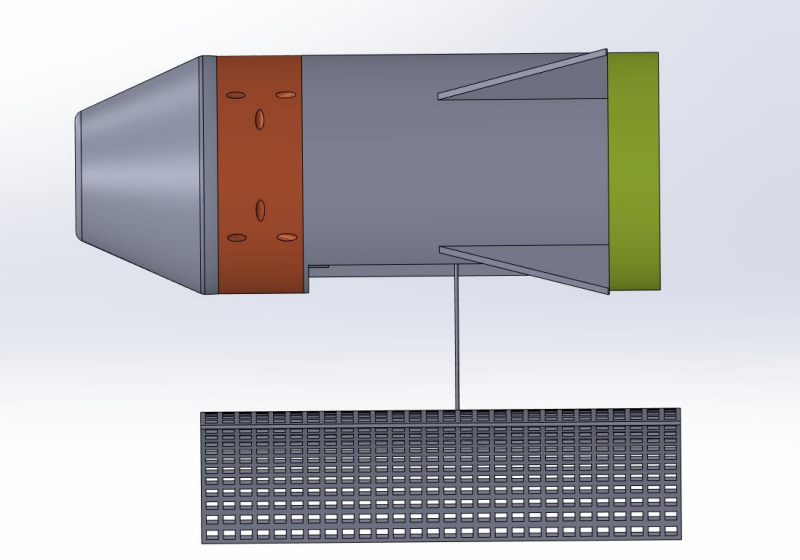

Figure 6-5- Capture net implementation (top view)

Last of all, the green part of the CAD model represents the docking port in which the spacecraft will exit and enter out of the ISS. This will be done through the implementation of the ELSA-d docking system which allows for continuous docking and undocking through magnetic means. More on the proposed use of the ELSA-d can be found in section 3 of this project.

6.3 Nose Section Design

For the nose section design, this section entails the design of the cockpit. The spacecraft is designed to sit three operators inside of the cockpit, with room overhead and below for storage of on-board batteries additional cargo. Rather than only having storage in the main cargo bay, additional storage spaces are placed near the cockpit for ease of access while the operator on board is still in the cockpit. Three console screens will be placed close to the seats for ease of control for all operators on board. Overall, the design aims to provide enough space for ease of usability and comfort for all operators on board. This is achieved through a wide nose cone that starts at around 5 meters at the base and tapers inwards.

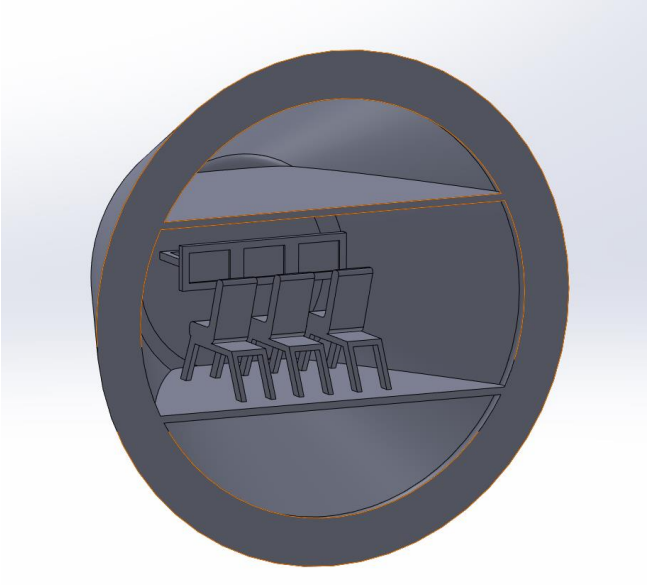

Figure 6-6 - Cockpit cutout (iso view)

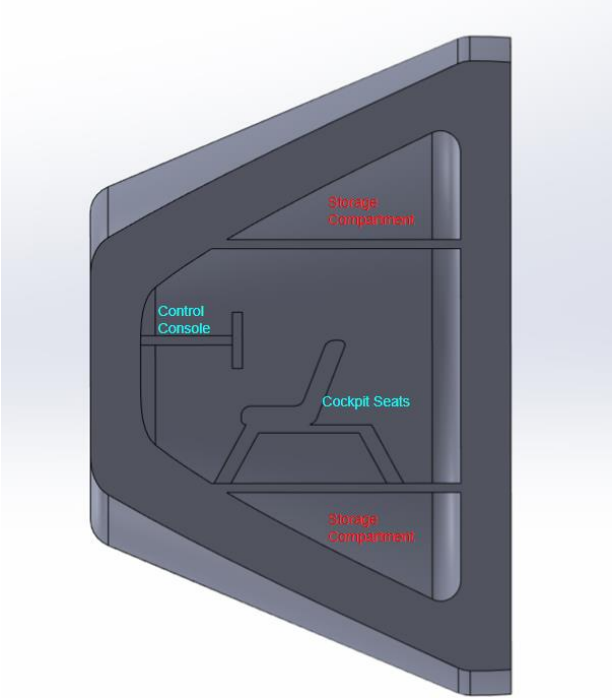

Figure 6-7 - Cockpit layout

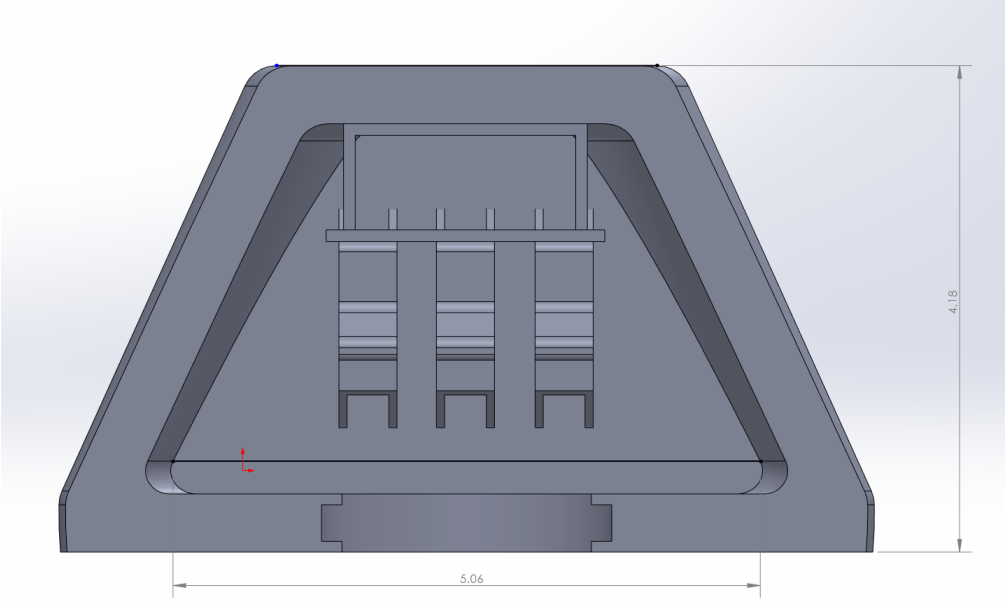

Figure 6-8 - Cockpit dimensions

7 Conclusion and Future Considerations

The adaptation of a method to reduce the amount of debris within the orbital atmospheres is crucial to the implementation of future space vehicles. This project aims to not only bring light to a quickly evolving problem within our orbital atmospheres, but also bring forth a solution that could mitigate the debris problem. This section will also highlight other future considerations and effects to consider when discussing the issue of space debris reduction

7.1 Collaborated Efforts

While this project offers a relatively easy solution of mitigating the issue of space debris, this spacecraft itself will not be enough to be a viable solution. This project aims to kick start the conversation and hopes to bring light the issue of space debris. To tackle this problem effectively, a total effort worldwide will be required to see measurable change. Every space program moving forward will need to start considering the waste that their respective projects produce and find ways of reducing their own waste that they exert into the atmosphere. As well as collaborated efforts across all space programs, additional laws could be put into place that will reduce the amount of debris in the atmosphere. However, because of the very aggressive nature of space discovery and travel, most projects aim to improve upon their project designs and goals at the expense of space. Therefore, an effort to reduce the debris in the atmosphere will be very unlikely soon.

7.2 Economic Considerations

Building a space debris removal spacecraft will be costly in terms of designing and implementing. A specialized docking mechanism will need to be installed and tested aboard the ISS and would be costly. Testing the capture net system will be of high importance, as testing on Earth will need to be done as well as testing in LEO to ensure functionality. Because this is the development and design of a new spacecraft, there will need to be new tooling made for the manufacturing of this project. The costs of keeping the spacecraft refueled as well as maintenance of other mechanical parts of the spacecraft will also need to be considered when implementing this project.

8 References

[1] “A Brief History of Space Debris”, Aerospace Corporation, November 2022 https://aerospace.org/article/brief-history-space-debris

[2] “National Orbital Debris Implementation Plan”, National Science and Technology Council, Executive Office of the President of the United States, July 2022 https://www.whitehouse.gov/wp-content/uploads/2022/07/07-2022-NATIONAL-ORBITAL-DEBRIS-IMPLEMENTATION-PLAN.pdf

[3] Balakrishnan, A., “U.S. Policies Relevant to Orbital Debris” IDA Science & Technology Policy Institute, October 2020

[4] Johnson, K., “Space Sustainability and Debris Mitigation” Key Governance Issues in Space, 2020, pp. 5-17

[5] Tallis, J., “Remediating Space Debris: Legal and Technical Barriers”, Strategic Studies Quarterly, vol. 9. 2015, pp. 86-99 https://www.airuniversity.af.edu/Portals/10/SSQ/documents/Volume-09_Issue-1/tallis.pdf

[7] “The TKS Transport Ship”, Russian Space Web, retrieved 21 February 2024. https://www.russianspaceweb.com/tks.html

[8] Rauf, J., “SpaceX Dragon Spacecraft”, University of Cincinnati, 2023 https://www.uc.edu/content/dam/refresh/cont-ed-62/olli/fall-23-class-handouts/SpaceX%205Dragon%20Capsules.pdf

[9] Johnson, G.,“Worldwide Spacecraft Crew Hatch History”, Science Applications International Corporation, National Aeronautics and Space Administration, October 2009

[10] “International Space Station”, ASEE Prism, vol. 8, No. 6, February 1999, pp. 8-9

[11] Mcfatter, J., Keiser, K., Rupp, T., “NASA Docking System Block 1: NASA’s New Direct Electric Docking System Supporting ISS and Future Human Space Exploration” Proceedings of the 44th Aerospace Mechanisms Symposium, NASA Glenn Research Center, May 16-18, 2018.

[12] “Nasa Docking System Technical Integration Meeting”, National Aeronautics and Space Administration, November 2010 https://web.archive.org/web/20130215180627/http:/dockingstandard.nasa.gov/Meetings/TIM_(Nov-17-2010)/NDS_TIM_presentation.pdf

[13] Gianini, G., “Electrical Propulsion in Space” Scientific American, vol. 204. March 1961, pp. 57-65

[14] Jahn R., “Electric Propulsion” American Scientist, vol. 52. June 1964, pp. 207-217

[15] Zucrow, M., “Space Propulsion Engines – Their Characteristics and Problems” American Scientist, vol. 50. September 1962, pp. 409-435

[16] Malik, T., “Praise Pours in for SpaceX Capsule’s Space Station Success”, May 2012, https://www.space.com/15880-spacex-praise-dragon-space-station.html

[17] Fouladinejad, F., Matkan, A., Hajeb, M., Brakhasi, F., “History and Applications of Space-Borne Lidars”, The International Archives of the Photogrammetry, Remote Sensing and Spatial Information Sciences, vol 42, October 2019

[18] Masetti, M., “Geoscience Laser Altimeter System (GLAS)”, National Aeronautics and Space Administration, January 2003
https://attic.gsfc.nasa.gov/glas/

[19] Saito, H., Tomiki, A., Mizuno, T., “High Bit-Rate Communication in X band for Small Earth Observation Satellites – Result of 505 Mbps Demonstration and Plan for 2 Gbps Link” 30th Annual AIAA/USU Conference on Small Satellites, 2016

[20] Rossi, A., Valsecchi, G., “The Space Debris Around Earth”, Science Progress, vol, 83. 2000, No. 4, pp. 337-355

[21] Wokes, S., Forshaw, J., Auburn, J., “ELSA-d: Mission Design and Performance to date”, ESA Clean Space Industrial Days, 2021
https://shorturl.at/govX3

[22] Benvenuto, R., Salvi, S., Lavagna, M., “Dynamics analysis and GNC Design of Flexible Systems for Space Debris Active Removal” Politecnico di Milano, Dipartimento di Scienze e Tecnologie Aerospaziali, Italy, 23 June 2014

[23] “SpaceX Draco” SpaceX Guide, retrieved 17 March 2024
https://spacex-guide.weebly.com/dracos.html

[24] Polk, J., Kakuda, R., Anderson, J., Brophy, J., “In-Flight Performance of the NSTAR Ion Propulsion System on the Deep Space One Mission” Jet Propulsion Laboratory California Institute of Technology, Pasadena, CA, February 2000

[25] Bond, T., Christensen, J., “NSTAR Ion Thrusters and Power Processors” National Aeronautics and Space Administration, November 1999

[26] Vozoff, M., Couluris, J., “SpaceX Products-Advancing the Use of Space”, American Institute of Aeronautics and Astronautics, San Diego, 11 September 2008

[27] “Pioneer F & G Final Report”, Teledyne Isotope Energy Systems Division, retrieved 20 September 2024,
https://digital.library.unt.edu/ark:/67531/metadc1027545/m2/1/high_res_d/4441003.pdf

[28] Miller, D., Keesee, J., “Spacecraft Power Systems”, Massachusetts Institute of Technology, retrieved 18 September 2024,
https://ocw.mit.edu/courses/16-851-satellite-engineering-fall-2003/2c8a1a136db0e366ae8d1a1e2995a505_l3_scpowersys_dm_done2.pdf

[29] Wertz, J., Larson, J.W., “Space Mission Analysis and Design”, Space Technology Library, vol 2. 1992

[30] “Space Observation Radar TIRA”, Fraunhofer Institute, retrieved 20 October 2024,
https://web.archive.org/web/20150501164108/http://www.fhr.fraunhofer.de/en/the_institute/technical-equipment/Space-observation-radar-TIRA.html

[31] “Basics of Spaceflight”, National Aeronautics and Space Administration, retrieved 18 October 2024,
https://science.nasa.gov/learn/basics-of-space-flight/chapter6-3/

[32] “48V WRO 14kWh Lithium Battery”, Shop Solar Kits, retrieved 20 November 2024
https://shopsolarkits.com/products/white-rhino-powerwall